Turbulence Modeling for Computational Aerodynamics

Joseph G. Marvin
NASA Ames Research Center, Moffett Field, California

Introduction

COMPUTATIONAL aerodynamics will have a significant role in the development of future aerospace vehicles.[1,2] Several key pacing items must be addressed, however, before its full potential can be realized.[3] Important among these is turbulence modeling, because the exact simulation of the dynamics of turbulence for practical applications is unattainable. Although new modeling concepts are being investigated, today's practical computations, and probably most of those that will be made in this decade, use the traditional modeling approach with some form of closure for the Reynolds-averaged[4] Navier-Stokes equations. This approach is taken with the expectation that studies of the deterministic structures of turbulence[5] and of numerical simulations of turbulence[6,7] will provide more understanding and eventually will guide the development of models that include more physical information.

Modeling in which traditional closure concepts are used eliminates important information about the dynamics of turbulence, and the universality of the approach has not been established. Therefore, limits of application must be determined by careful comparison with well-conceived experiments. Progess in that direction was reported for incompressible boundary-layer flows in the late 1960's.[8] During the last decade, however, advances in computational aerodynamics have increased our ability to compute more complex flows markedly, and the burden of establishing limits of applicability for turbulence modeling has increased proportionately.

The recent AFOSR/HTTM-Stanford Conference[9] is witness to the breadth of that task. The scope of that conference was broad and there was no particular emphasis on external aerodynamic flows, as there is in this paper. For those unfamiliar with the progress and direction of the modeling of external flows, this paper will provide a perspective from which to view further developments certain to come in the next decade. For those entering the field of computational aerodynamics and who are interested in using various models in their computations, it will provide a basis of reference and, it is hoped, help them avoid unnecessary difficulties. For those active in the field, it will simply reinforce what they already know about the problems of modeling, although it may also suggest some new ways to view combined computational and experimental investigations.

A complete review of modeling, even within the closure framework for the Reynolds-averaged Navier-Stokes equations, is beyond the scope of this paper, and the reader is referred to several excellent books[10-12] that review the development of modeling and give details on the formulations of various models. This discussion is limited to a few important external aerodynamic flows of practical interest. Many of the examples, familiar to the author and to his colleagues, were chosen because the author had first-hand access to information about them, and because it is believed that they are a fair representation of the broader spectrum of today's modeling activities.

Modeling Concepts for Compressible Flows

Many of the practical aerodynamic flows of interest occur at speeds at which compressibility effects must be included. The first task, then, is to develop appropriate governing equations before the modeling concepts are discussed.

Governing Equations

The governing equations describing the fluid motion are the compressible form of the Navier-Stokes equations. Following Reynolds,[4] the variables are expressed in terms of their time-averaged values ($\bar{}$) and their fluctuations ( )″, and the equations are averaged over a time that is long compared with that of the predominant turbulence frequencies. Complications arise immediately. The continuity and momentum equations contain fluctuating density-generated terms, such as $\rho'' u_m''$, that must be modeled in addition to the usual Reynolds stresses, $\bar{\rho} u_i'' u_j''$. Donaldson and his co-workers use equations derived in this manner, and they have developed an invariant Reynolds stress model[13] requiring modeling for 41 closure moments. However, most investigators avoid these difficulties by introducing mass-weighted, or Favré, averaging.[14] The resulting equations are as follows:

Continuity:

$$\frac{\partial \bar{\rho}}{\partial t} + \frac{\partial}{\partial x_j}(\bar{\rho}\tilde{u}_i) = 0 \tag{1}$$

Momentum:

$$\frac{\partial}{\partial t}(\bar{\rho}\tilde{u}_i) + \frac{\partial}{\partial x_j}(\bar{\rho}\tilde{u}_i\tilde{u}_j) = -\frac{\partial \bar{p}}{\partial x_i} + \frac{\partial}{\partial x_j}(\bar{\tau}_{ij} - \overline{\rho u_i' u_j'}) \tag{2}$$

Joseph G. Marvin is chief of the Experimental Fluid Dynamics Branch at Ames Research Center. The branch was formed in 1972 and performs combined experimental and computational research in space vehicle aerothermodynamics and turbulence modeling. Marvin, a graduate of Santa Clara and Stanford Universities, came to Ames in 1956. His research has included work on re-entry heating, planetary entry heating, boundary-layer transition, Space Shuttle aerothermodynamics, and turbulent flows with emphasis on separation and Reynolds number effects for the transonic and supersonic speed regimes. He was a member of the NASA Boundary-Layer Transition Study Group and the NASA Shuttle Aerothermodynamic Heating Panel; was responsible for the hypersonic aerothermodynamic wind tunnel test program at Ames supporting the Space Shuttle development; is an Associate Fellow of the AIAA; is a State of California registered professional engineer; and is a reviewer for *Applied Mechanics Reviews*.

Presented as Invited Paper 82-0164 at the AIAA 20th Aerospace Sciences Meeting, Orlando, Fla., Jan. 11-13, 1982; submitted Jan. 22, 1982; revision received Sept. 10, 1982.

Energy:

$$\frac{\partial}{\partial t}\bar{\rho}\tilde{h}+\frac{\partial}{\partial x_j}(\bar{\rho}\tilde{h}\tilde{u}_j)=\frac{\partial\bar{p}}{\partial t}+\tilde{u}_j\frac{\partial\bar{p}}{\partial x_j}+\overline{u_j'\frac{\partial p}{\partial x_j}}$$
$$+\frac{\partial}{\partial x_j}(-\bar{q}_j-\overline{\rho h' u_j'})+\overline{\tau_{ij}\frac{\partial u_i'}{\partial x_j}} \tag{3}$$

where u_i and x_i are the velocity and its direction, respectively; ρ the density; p the pressure; h the enthalpy; and τ_{ij} and q_j the instantaneous molecular shear stress and heat flux, respectively. The bars and primes denote the usual time-averaged and fluctuating values, and the tildes denote the mass-weighted averaged values. These equations have the same form as the incompressible time-averaged equations, except that the Reynolds stresses, $\overline{\rho u_i' u_j'}$, include fluctuations in density which must be accounted for in some manner.

The governing equations can be supplemented by additional equations for the turbulent kinetic energy k and the various Reynolds stresses. These may be written as[14]

Turbulent kinetic energy:

$$\frac{\partial}{\partial t}(\rho k)+\frac{\partial}{\partial x_j}(\rho\tilde{u}_j k)=-\overline{\rho u_i' u_k'}\frac{\partial\tilde{u}_k}{\partial x_k}-\frac{\partial}{\partial x_k}\overline{\rho u_k' k}-\frac{\partial}{\partial x_i}(\overline{u_i' p})$$
$$+p\overline{\frac{\partial u_i'}{\partial x_i}}+\frac{\partial}{\partial x_k}\overline{u_i'\tau_{ik}}-\overline{\tau_{ik}\frac{\partial u_i'}{\partial x_k}} \tag{4}$$

Reynolds stress:

$$\frac{\partial}{\partial t}(\overline{\rho u_i' u_j'})+\frac{\partial}{\partial x_j}(\tilde{u}_j\overline{\rho u_i' u_k'})=(\overline{\rho u_i' u_j'})\frac{\partial\tilde{u}_k}{\partial x_j}-(\overline{\rho u_k' u_j'})\frac{\partial u_i}{\partial x_j}$$
$$-\frac{\partial}{\partial x_j}(\overline{\rho u_i' u_k' u_j'})-\frac{\partial}{\partial x_j}(\overline{u_i' p})-\frac{\partial}{\partial x_k}(\overline{u' p})+p\overline{\frac{\partial u_k'}{\partial x_i}+\frac{\partial u_i'}{\partial x_k}}$$
$$+\frac{\partial}{\partial x_j}(\overline{u_k'\tau_{ij}})+\frac{\partial}{\partial x_j}(\overline{u_i'\tau_{ki}})-\overline{\tau_{ij}\frac{\partial u_k'}{\partial x_j}}-\overline{\tau_{ki}\frac{\partial u_i'}{\partial x_j}} \tag{5}$$

The conservation and supplemental equations have unknowns that exceed the number of equations. Reducing the number of unknowns to the number of equations is called the "closure" problem. Expressing the unknowns as transport equations or functions in terms of known quantities is called turbulence modeling.

Modeling Concepts

Modeling concepts (Fig. 1) are classified as either eddy-viscosity or Reynolds-stress models. Features that distinguish models of either class or models within the same class arise through the particular closure technique that expresses the modeled quantities in terms of the mean-velocity field or in terms of the mean-turbulent field. Techniques for implementing the closure vary widely. Herein details are omitted and only the main points are outlined to provide continuity to the discussions that follow.

Eddy-Viscosity Models

The eddy-viscosity models invoke Boussinesq's idea.[15] The turbulent shear stresses in the mean-momentum equations are replaced by the product of an effective viscosity and a mean rate of strain. They are often referred to as zero-, one-, and two-equation models,[16] in reference to the number of supplementary equations, beyond the usual mean conservation ones, used to effect closure. Thus, zero-equation models are those that rely on specifying velocity and length scales in terms of the mean flow. One- and two-equation models obtain the velocity scale from a solution of the modeled form of the turbulent kinetic energy equation and a specified length scale in the one-equation approach or a solution of a modeled length scale equation in the two-equation approach. In contrast to the zero-equation models, which imply an equilibrium between the mean motion and the turbulence, these higher order models are intended to apply more appropriately in situations in which the mean motion and turbulence are not in equilibrium.

For zero-equation models, compressibility is simply introduced by using the local mean density in the definition of eddy viscosity and neglecting higher order correlations in the definition of the turbulent shear stress. Following Morkovin's hypothesis[17] that compressibility should not affect the description of the length scales, the constants used are usually those developed for incompressible applications. Such assumptions seem to work well up to Mach numbers of about 5 for attached boundary layers.

The compressible form of the turbulent kinetic energy and shear-stress equations contains additional correlations that arise because of compressibility. The modeling of these equations has been carried out formally.[18,19] In practice the additional modeling terms have little influence[20] and they are usually dropped; however, this particular aspect may warrant further investigation, especially when flows involving strong shock waves are present or when the flow is hypersonic. Also, as for zero-equation models, modeling constants derived for incompressible flows have usually been used.

Stress-Transport Models

Stress-transport models use the Reynolds-stress equations to provide the turbulent stresses in the mean-momentum equations. Their advantage over the eddy-viscosity models is that they remove the assumption that the stresses respond immediately to changes in the strain rate. The complexities of modeling at this level, however, have led to approximate methods, as outlined in Fig. 1. The simplest is a model that uses a single equation—the turbulent kinetic energy equation—and invokes a proportionality observed experimentally that relates this energy to the shear stress.[21] Another uses two equations: the turbulent kinetic-energy

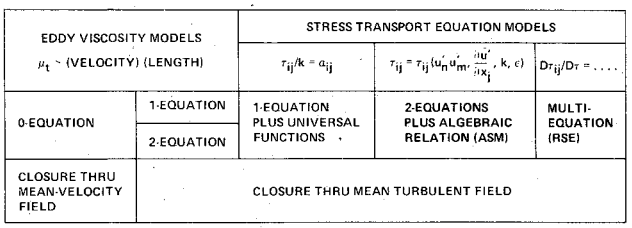

Fig. 1 Outline of turbulence modeling concepts using single-point closure.

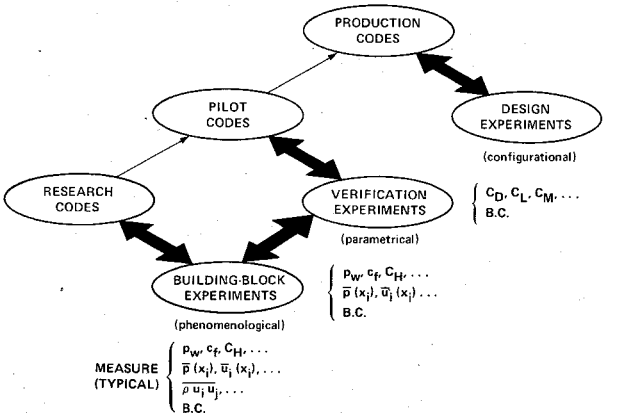

Fig. 2 Framework for advancing computational aerodynamics.

equation and a scale equation. Algebraic relations relate the stresses to these (e.g., Ref. 22). Finally, there are full Reynolds-stress models[13,23] that solve equations for each of the stresses.

Compressibility is included in the models by introducing mean density when mass-averaged variables are used; terms involving additional correlations arising from compressibility are neglected.[23] As mentioned previously, Donaldson, who uses time-averaged variables, models the correlations involving density fluctuations.[13] Modeling coefficients derived from incompressible flows usually have been used. The choice of what closure level to use will depend on the problem under consideration and on the information required from the computation.

Experiments Supporting Modeling Development

The emergence of methods for computing complex viscous flows has placed stringent requirements on experiments supporting development of turbulence modeling. In addition to increasing the basic understanding of fluid motions, these experiments must provide input for modeling approximations and evaluation and provide precise checks on computational output. A number of experiments were evaluated recently and selected for this purpose.[9] Although they encompass a wide range of flow types and conditions, those selected that pertain to external aerodynamic flows comprised only a small part of the total. Furthermore, the accuracy of even the best of the experiments is uncertain because measurements at the speeds and Reynolds numbers of interest are more difficult. Because there is an obvious need for more experiments, it is appropriate to outline some of the important experimental requirements so that future experiments will provide the elements essential to modeling guidance and verification.

Experimental Requirements

A convenient framework for discussing experimental requirements is illustrated in Fig. 2. Experiments are considered keyed directly to three stages of development of computational aerodynamics: research codes, pilot codes, and production codes. For example, the ability to compute certain

Table 1 Bibliographic survey of modeling activities supporting computational aerodynamics[a]

Flow type/ modeling issue	Supporting experiments	Computation framework/turbulence model							
		Boundary-layer equations				Navier-Stokes equations			
		0-Eq.	0-Eq. mod.	2-Eq.	τ_{ij}	0-Eq.	0-Eq. mod.	2-Eq.	τ_{ij}
Attached: 2-D									
Averaging	25	27	...	27	27	...	...	...	...
Mach No. effects	25,26	27	...	23,27,28	23,28	...	...	9	...
Reynolds No. effects	25,26,30	29	...	29	...	...	...	...	...
Pressure gradient	26,30	27	31-33	27	28	...	...	...	...
Curvature	26,34,35	...	36-38	...	...	...	...	...	...
Attached: 3-D									
Isotropic eddy viscosity	39-44,48,51	45-48	...	40,45,46,48	...	...	...	...	...
Anisotropic eddy viscosity	39-44,49,51	...	40,45,47,49	40,45,50	...	...	...	...	...
RSE development	39-44,49,51	...	...	...	45,48-50,52	...	...	...	...
Compressibility	42,43,53-55	54,56	...	...	...	55	...	53	...
Separated/reattaching									
2-D Shock-induced									
Isotropic eddy viscosity	57-65	60,63,67	66,67	...	...	60,62,64 68-73	68,70-72 74	60,64,69 72,73,75-77	...
2-D Geometry-induced									
Isotropic eddy viscosity	9,78,79	...	...	...	...	...	...	9,82	...
RSE development	9,78,79	...	...	...	...	...	...	...	9,82
2-D Pressure-induced									
Isotropic eddy viscosity	9,80,81,83	9,80,81	...	9,80	...	...	...	...	...
3-D Shock-induced									
Isotropic eddy viscosity	84-88	...	...	...	...	87	9,86,88,89	...	
3-D Cross-flow									
Isotropic eddy viscosity	90	...	...	...	...	91,92	91	...	...
Anisotropic eddy viscosity	...	...	...	...	...	...	91	...	...
Trailing edge									
2-D, no pressure gradient									
Near-wake development	93-96	...	97	9,93,95	9	...	...	...	...
2-D, adverse pressure gradient									
Near-wake development	98-104	...	...	6,93	9	97,88	...	98,99	102,105
3-D, adverse pressure gradient									
Near-wake development	45	...	45	45	45	...	...	...	...

[a] Numbers designate references.

flow phenomena is established in the research phase. Building-block experiments, which provide phenomenological modeling information, are needed at this stage. More efficient pilot codes are developed next; they extend the applications of the research codes to a wider range of conditions or to different geometries. Verification experiments, which provide parametric information, are needed at this stage. The third stage, in which production codes are developed for design applications, is not pertinent to this discussion of modeling; nonetheless, it is shown in Fig. 2 for completeness. Experiments that address optimal configurational performance are needed at this stage.

Each of these experimental stages must provide specific information for guidance and critical assessment of the computer codes. Key requirements for each category are discussed in Ref. 24 and are noted in Fig. 2. Building-block experiments must document sufficient information on flow phenomena to provide modeling guidance and to provide a critical test of the codes' performance. Surface variables and flow variables, including turbulence information, are essential, and measurements are required at test conditions representative of flight Mach numbers and Reynolds numbers. Verification experiments must provide sufficient information to test the ability of codes to perform adequately over a range of flow conditions or for a variety of configurations. At this stage of development, detailed information on flow modeling is not essential, but parametric testing over the full range of flight Mach numbers and Reynolds numbers is essential. Code failures at this stage may require that additional building-block experiments be defined and performed. Design experiments provide the optimal configuration data necessary for performance evaluation and must be carried out as close to flight conditions as practical. Boundary-condition specifications are important at all stages because they may influence the flowfield around test models; moreover, they are often required to initiate computations or are approximated in the numerical solution. Future experiments planned with this framework in mind should help to accelerate the development of modeling for computational aerodynamics.

Test Flows

Modeling concepts are being developed and assessed against experiment mainly by using research computer codes. These are boundary-layer codes and Reynolds-averaged Navier-Stokes codes. The corresponding experiments are mostly of the building-block variety. A summary of activities reviewed by the author during preparation of this paper is shown in Table 1. It provides a partial bibliographic guide (Refs. 25-105) and serves as an outline of the presentation that follows.

The test flows are divided into three broad types that are of practical interest in external aerodynamic applications: 1) attached flows, 2) separated and reattaching flows, and 3) trailing-edge flows. Some important modeling issues are listed for each flow type. Experiments that can serve as test flows are listed by reference number. The type of data and their accuracy vary considerably. Not all the data sets have been evaluated in the manner used by the organizers of the AFOSR/Stanford Conference,[9] and it is not recommended that any single experiment be used as the sole basis for model development. References in which comparisons with data are reported are listed according to computational framework and models tested. Integral and interactive methods of computation have been omitted for conciseness, but references germane to modeling studies are listed under the boundary-layer computation framework.

Comparisons of Experiment and Computations

The status of modeling will now be reviewed by discussing comparisons of experiment and computation for some selected test flows.

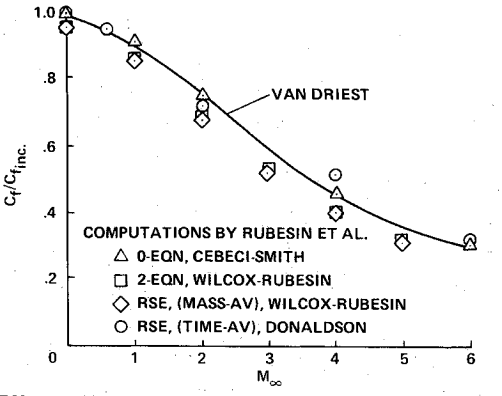

Fig. 3 Effects of compressibility on turbulent skin friction on a flat plate: adiabatic wall, $Re_L = 10^7$.

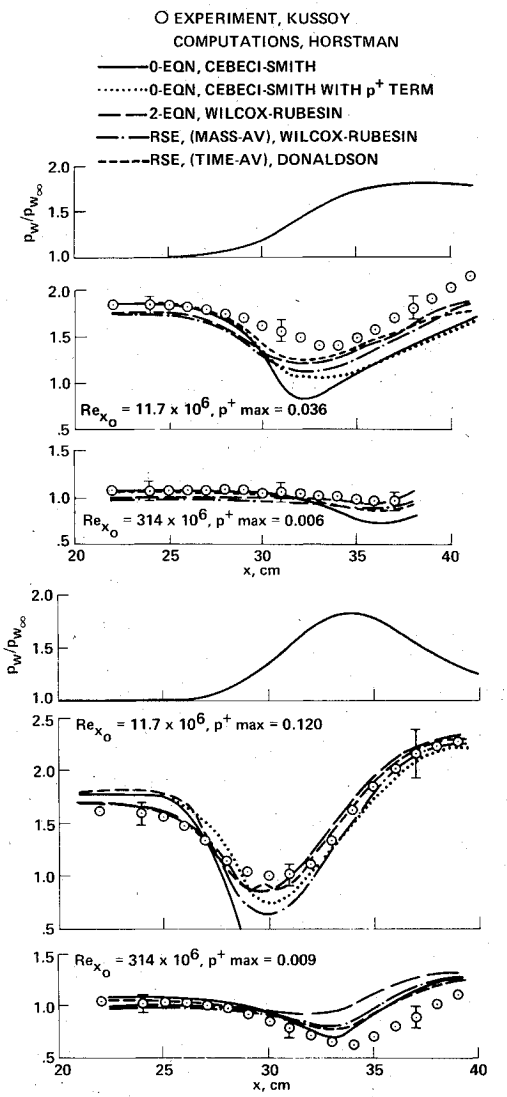

Fig. 4 Effects of pressure gradient and Reynolds number on a compressible turbulent boundary layer, $M_\infty = 2.3$: a) adverse pressure gradient to a plateau; and b) adverse pressure gradient followed by a favorable one.

Attached Flows

Two-Dimensional Flows

These flows can be used to address the issues involved in extending models developed for incompressible flows to the compressible regime associated with flight Mach numbers and Reynolds numbers of interest in aerodynamic applications. The discussion is limited to Mach numbers below 6.

The effect of compressibility on skin friction for a flat-plate, turbulent boundary layer is shown in Fig. 3. The Van

Driest prediction[25] represents available data to within 10% and can be considered a standard for comparison with prediction. Computations[23,27] in which the boundary-layer form of the Reynolds-averaged equations are used with various classes of models are compared with it. Aside from showing that all models predict the trends of compressibility with a reasonable accuracy, several important conclusions can be drawn. The choice of mass-weighted- or time-averaging has no significant effect on the predicted results using models that employ the mean turbulent-field equations for closure. The two-equation model and the Reynolds stress equation (RSE) model due to Wilcox and Rubesin consistently predict lower values of skin friction. The zero-equation, Cebeci-Smith model[11] reproduces the Van Driest result more accurately; if turbulence information is not needed, this model would have to be the choice for predictions, considering its simplicity. Similar results have been obtained for cool-wall cases.[23]

A more difficult test of the models occurs when extra strain rates, such as those introduced by a pressure gradient and surface curvature and which are of practical interest in many aerodynamic flows, are present.

Comparisons of predictions[29] and experiment[30] for a wide range of Reynolds number and various pressure gradients are given in Ref. 29 and some typical results are shown in Fig. 4.

In the first example (Fig. 4a), an adverse pressure gradient whose magnitude is characterized by the pressure gradient parameter, $p^+ = \rho_w \mu_w (dp/dx)/\tau_w \rho_w)^{3/2}$, is imposed on a flat surface over a distance of about 5 upstream-boundary-layer thicknesses, and the pressure remains constant thereafter. As the Reynolds number increases, the imposed pressure distribution remains fixed while the skin friction changes significantly. The calculations were initiated by matching the experimental displacement thickness δ^* at an initial data station; small differences in the initial skin friction, similar to those shown in Fig. 3, result for the various models. All the models predict the general trends of the experiment, but they tend to overestimate the influence of the pressure gradient. The zero-equation Cebeci-Smith model (solid line, Fig. 4) is the most obvious in this regard, but the p^+ correction recommended by the model originators[11] (dotted line) tends to correct this. The models that use the mean-field turbulent equations for closure appear to give better predictions without requiring that modeling coefficients be modified to account for pressure gradient.

For the second case (Fig. 4b) the adverse pressure gradient is somewhat higher, and it is followed by a region of favorable pressure gradient. In this instance, the zero-equation model is deficient, and, without modification for pressure gradient, it predicts separation at the lowest Reynolds number. Also, all the models tend to underestimate the Reynolds number effects in the downstream region where the favorable pressure gradient is present.

Longitudinal surface curvature becomes important when the gradient Richardson number, $2U/R/\partial u/\partial y$, is approximately 0.1. Development of turbulence models that account for curvature effects has been carried out for incompressible flows.[23,34,38] The models that achieve closure through the mean-turbulent-field equations[23] apparently yield better results for the cases with combined effects of pressure gradients and curvature. The author is unaware of similar developments for higher speed ranges. Based on the results from the previous examples, however, extension of the models to the compressible regime should be straightforward and probably yield adequate predictions.

The comparisons for attached flows establish that all models predict the observed data trends well enough to provide estimates of viscous effects that are accurate enough for engineering purposes. Models that effect closure through the mean-turbulent-field equations appear to be more generally applicable, and they offer the best prospects for predictability outside the range of available experiment; however, they are more difficult to use and are less efficient computationally. For these reasons, some investigators have attempted to modify the zero-equation models. The most popular of these is referred to as a relaxation or lag model, because it uses simple ordinary differential or algebraic equations to modify modeling constants (see, e.g., Refs. 31-33). When employed outside the range of the experimental data used to develop them, however, these modifications must be applied with caution.

Three-Dimensional Flows

The question of how well the models that were developed for two-dimensional attached flows apply to three-dimensional flows is addressed next. The incompressible test flow of Elsenaar et al.[39] was chosen as a typical example, since it has many of the flow features encountered on wings and has been used by various investigators to evaluate modeling concepts. The flow was established over a swept flat plate in a manner that developed similar to that expected on a wing of infinite aspect ratio. An upper-tunnel-wall modification provided an adverse pressure gradient that led to separation; separation is defined as the location where the local surface-shear component in the freestream direction approached zero. The resultant flow encompasses a range of cross flows.

Comparisons of skin friction and surface turning angle obtained from unpublished boundary-layer calculations employing three turbulence models are given in Fig. 5. The zero- and two-equation solutions assume an isotropic eddy viscosity; both predict the initial portion of the flow where the boundary-layer skewing angle β_w is less than 15 deg, but both fail for larger angles. The experimental velocity and shear-stress profiles were interpreted, and it was suggested that an anisotropic eddy viscosity might be more appropriate.[39] An analysis by Rotta,[50] using a limiting form of the Reynolds-stress equations provides a rational basis for using the anisotropic eddy viscosity; attempts to improve the predictions accordingly were made (see, for example, Ref. 45). Such improvements require experiment-dependent input, however, and the results are about the same as those shown in Fig. 5 for the full Reynolds-stress model, which is less ambiguous in application but more costly in computational time. The shortcomings in the Reynolds-stress solution probably result from modeling the pressure-strain correlations and the low-Reynolds-number formulation in the vicinity of the wall.

The effects of transverse strain on a turbulent boundary layer, in the absence of pressure gradient, is under study[48] to provide guidance for modeling the pressure-strain correlations and the low-Reynolds-number terms in the Reynolds-stress model used in the previous example. The authors report results using several different pressure-strain correlation models, but none yet shows significant improvement and further studies are proceeding. These examples and others not discussed here, including those for swept wings at transonic speeds[53,56] and bodies of revolution at supersonic speeds,[54,55] suggest that isotropic eddy-viscosity models are only adequate for predicting flows with moderate cross flows. It is apparent that much remains to be accomplished in modeling for the case of significant cross flow. As is so often the case with complex flows, however, it is not entirely clear whether the differences between experiment and computation for large cross flows are entirely caused by turbulence modeling. Experimental accuracy and computational techniques are also likely to contribute to differences. In the swept-plate flow, for example, boundary-layer theory is applied when normal pressure gradients are present, especially near the rear of the plate; moreover, the calculations themselves are extremely sensitive to small changes in external velocity gradient, changes that are within acceptable data accuracy tolerance. Therefore, additional test flows and comparisons will be needed to help establish the status of modeling. In that regard it should be noted that the

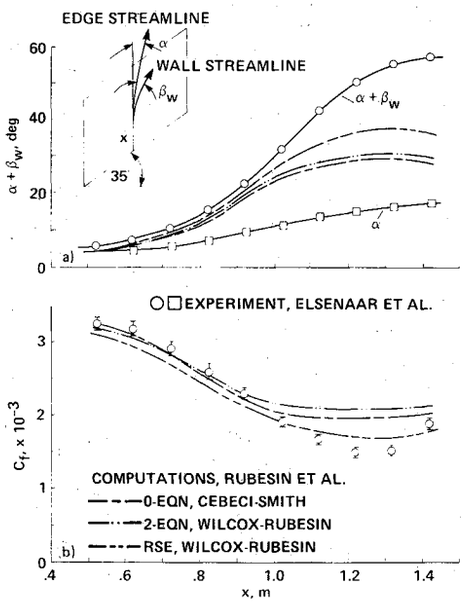

Fig. 5 Variation of skin-friction and wall shear-stress direction on an infinite swept plate with adverse pressure gradient: a) wall shear-stress direction; and b) skin friction.

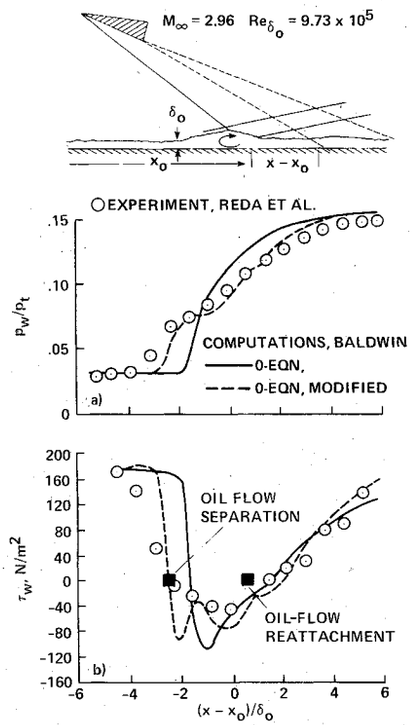

Fig. 6 Comparison of predicted and experimental data for a shock-separated flow: a) pressure ratio; and b) wall shear-stress.

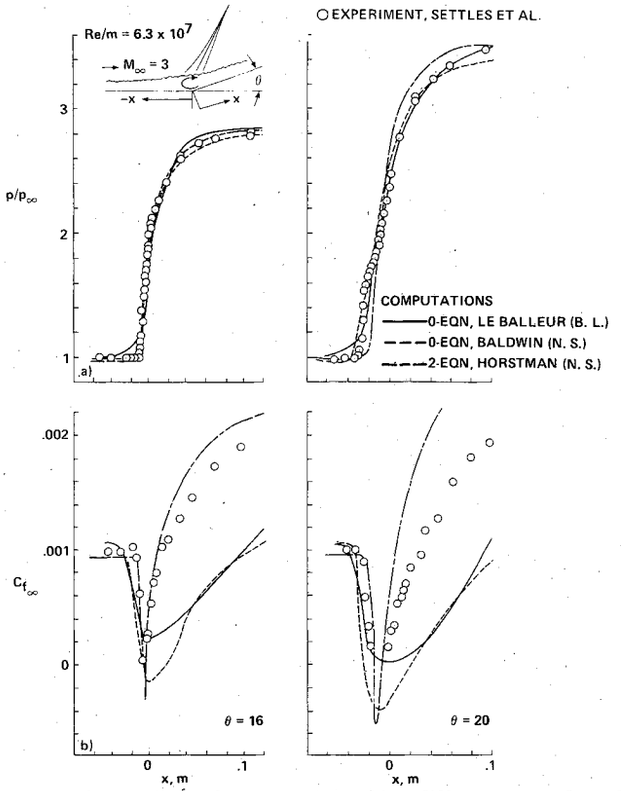

Fig. 7 Comparison of computations using different methods and models with experiment for a compression corner: a) surface pressure; and b) skin friction.

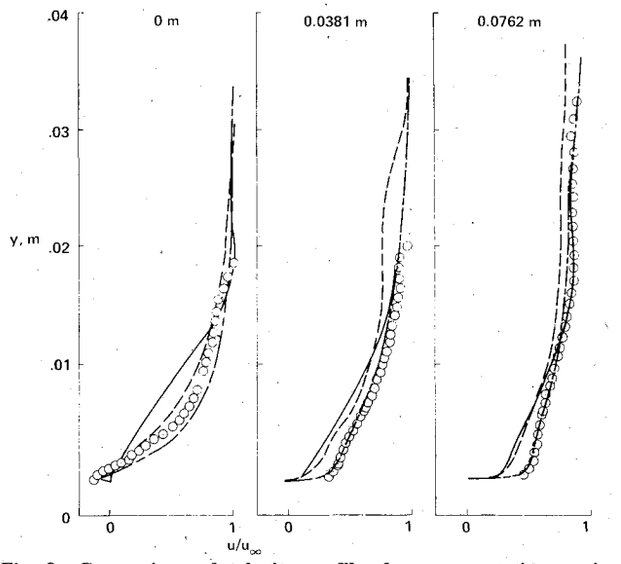

Fig. 8 Comparison of velocity profiles from computations, using different methods and models with experiment for a compression corner (see Fig. 1 for symbol notation).

proceedings of the IUTAM workshop on three-dimensional flows, held in Berlin, FRG, and edited by E. Krause et al. should become available soon.

Separated and Reattaching Flows

Two-Dimensional Flows: Shock Waves

There was an increase in numerical modeling of two-dimensional flows with shock waves following the solution to the laminar separation problem by MacCormack.[106] As shown in Table 1, most of the studies of turbulence modeling use codes that solve the Reynolds-averaged form of the Navier-Stokes equations. Early studies used zero-equation models because the solution convergence times were excessive. As algorithms and convergence times were improved, eddy-viscosity models that achieve closure through solutions of the mean-turbulent-field equations were studied. The following examples illustrate the essential results of these studies. No solutions with Reynolds-stress models have yet been attempted.

The separation caused by a shock impinging on a supersonic turbulent boundary layer was one of the first problems attempted. An example of one test flow is shown in Fig. 6 along with comparisons of computation[70] and experiment.[59]

This particular experiment was not recommended as a test flow for the recent AFOSR/Stanford Conference because it has three-dimensional effects present, but it does serve to illustrate attempts at improving zero-equation models. As shown in Fig. 6, the zero-equation Cebeci-Smith model predicted neither the pressures nor skin friction satisfactorily, although it did reproduce, qualitatively, all the essential features of the flow (e.g., separation, reattachment, and a reflected shock). However, the calculated separation bubble height was too small, and its forward influence on the oncoming boundary layer was negligible, because the modeled eddy viscosity in the interaction region was too large. There were attempts to modify the model by using an algebraic relaxation equation[70] for the outer eddy viscosity, and, indeed, a plateau in pressure was predicted, there was more forward influence, and a better representation of the skin friction was obtained. However, the results depended on the choice of the relaxation length, and other computations for other flows suggested that the optimum length differed from flow to flow. As a result, it seems that the search for a general zero-equation relaxation model has been dropped. For the same reasons, modifications to modeling coefficients, such as A^+, the Van Driest damping coefficient, and κ, the Karman constant, which also were effective in achieving better predictions for shock impinging flows,[68] have not been pursued.

Although turbulence modeling was often cited as the main deficiency in these early computations, the algorithm, grid, convergence criteria, and the experiment itself were also contributing factors. The effects of these latter factors are probably minimized in the example that follows—a test flow that is a supersonic compression corner, chosen as one of the cases for the recent AFOSR/Stanford Conference.[9] The experimental data[65] were checked closely and judged by an evaluation committee to be accurate enough for model evaluation purposes.

Comparisons of computation and experiment are given in Fig. 7. Results from three calculations are shown, two obtained from solutions of the Navier-Stokes equations and one from an inviscid-viscid interactive scheme employing an integral boundary-layer method.

In the interactive solution of LeBalleur and the Navier-Stokes solution by Baldwin, zero-equation eddy-viscosity concepts are used. The Navier-Stokes solution by Horstman uses the Wilcox-Rubesin two-equation model. In earlier studies,[107] Baldwin found it necessary to modify the zero-equation model outer eddy-viscosity formulation, because uncertainties in locating the outer edge of the boundary layer can introduce large errors in the length-scale determination. LeBalleur et al.[66] used a Prandtl-Meyer approximation for the inviscid outer flow. In the viscous region he used an algebraic relaxation equation, derived from the integral form of the turbulent kinetic energy equation, to account for nonequilibrium effects on the entrainment equation. The investigators reported using very fine grids that were sufficient to resolve the viscous flow features, and they used the experimental boundary conditions.[9] Convergence was considered achieved when successive iterates produced minor changes in the pressure distribution. Differences, then, are mainly attributable to modeling. An obvious observation is that all the computations reproduce the overall character of the experimental pressures reasonably well for the two deflection angles corresponding to incipient separation ($\theta = 16$ deg) and full separation ($\theta = 20$ deg), indicating that the turning of the flow is dominated by inviscid effects. Other differences are attributable to the viscous portions of the calculations and are due to the different models. The Navier-Stokes solutions fail to give a significant plateau for the fully separated case, an indication that the eddy viscosities are probably too high and that the bubble height is too small. The addition of the lag equation in the integral solution apparently improved this somewhat. The corresponding calculations for the skin friction show widely differing results. The zero-equation predictions underestimate the skin friction along the deflected wall, and the two-equation model prediction overestimates it. Nevertheless, the two-equation model gives a much better representation of the developing flow along the wall, as shown by comparisons with the velocity profile data in Fig. 8. Also, although not shown here, this model predicts the correct Reynolds number trends on separation and reattachment locations whereas the others do not. None of the models has been modified for curvature effects (which could be important).

Another comparison is shown in Figs. 9 and 10. A low-Mach-number supersonic flow was established inside a circular test section and a shock wave that interacted with the wall boundary layer was formed, using a downstream choking device. Measurements[64] were taken over a range of Mach numbers between 1.3 and 1.44 and over a range of Reynolds numbers between 8×10^6 and 200×10^6. The pressure and skin friction from solutions of the Reynolds-averaged Navier-Stokes equations,[72] using two eddy-viscosity models, are compared with the experimental data for one Mach number

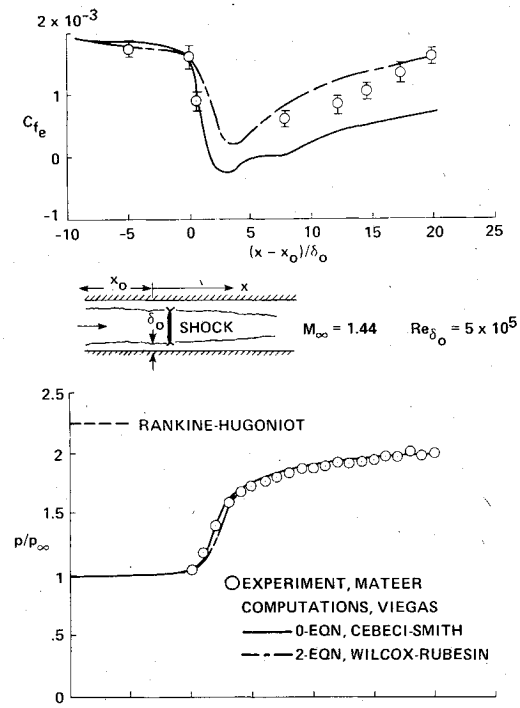

Fig. 9 Comparison of computation and experiment for a transonic normal shock-wave interaction: a) wall pressure; and b) skin friction.

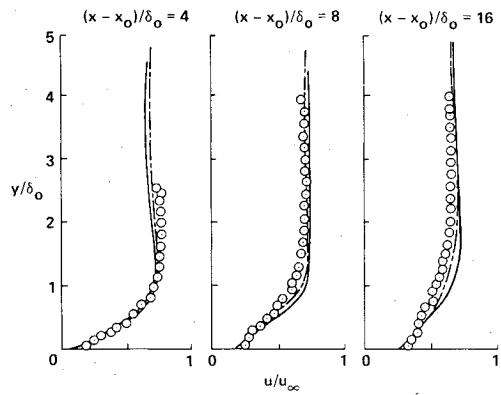

Fig. 10 Comparison of computation and experiment for a transonic normal shock-wave interaction: velocity profiles (see Fig. 9 for symbol notation).

and one Reynolds number. Separation in this test flow is small. As in the previous example, the pressure distribution is predicted when either model is used, but better skin-friction distributions and velocity-profile development are obtained downstream of reattachment with the two-equation model that achieves closure through the solution of the mean-turbulent-field equations. Similar comparisons are available over the complete Mach and Reynolds number ranges of the experiment.[64]

In the preceding examples, the location of the shock wave was essentially "fixed" in the flowfield by geometrical or pressure-ratio constraints. For such flows, pressure distributions are predicted fairly well, using any of the eddy-viscosity models, apparently a result of the inviscid-dominated nature of the outer part of the flows. On the other hand, the skin friction, a measure of how the viscous stresses are being modeled, is not predicted as well. This points out several modeling deficiencies, the most obvious of which is the failure of zero-equation models to predict the proper skin friction and corresponding velocity profiles in the developing boundary layer downstream of the interaction; the two-equation models show improvement in this regard. None of the models shows the proper upstream influence of the interaction when separation is large; moreover, the models usually fail to predict the separation point, probably because of their inability to model the proper height of the separation bubble. Although these discrepancies may be acceptable in some practical applications for fixed shock problems (because the interaction zone represents only a small region of the flow), they have a strong influence on modeling of transonic flows with large separation, where shock-wave position depends on the elliptic character of the flow.

The transonic "axisymmetric bump" experiment,[60] evaluated and chosen as a test flow for the AFOSR/Stanford Conference,[9] will illustrate the problem. A strong shock and separation similar to that on an airfoil is developed. The experimental results are compared in Fig. 11 with Reynolds-averaged Navier-Stokes solutions[60] employing zero- and two-equation models. In contrast to the previous examples, the pressure distribution is not predicted, except downstream of the shock wave in the reattachment region and beyond. The largest disagreement in pressure distribution occurs near the shock wave, which is predicted to be too far downstream. This result is typical of comparisons for other transonic flows on airfoils (see, for example, Refs. 62 and 71). Although surface-curvature effects have not been included, the discrepancies are most probably related to the inability of the models to predict the proper upstream influence caused by separation on the oncoming boundary layer ahead of the shock wave. When this influence is absent, the shock position is farther downstream and an abrupt increase in the turbulent stresses is predicted.

Comparisons of the computed and measured velocity and shear-stress profiles (Fig. 12) show that the maximum shear and its location in the flow are predicted quite well by either

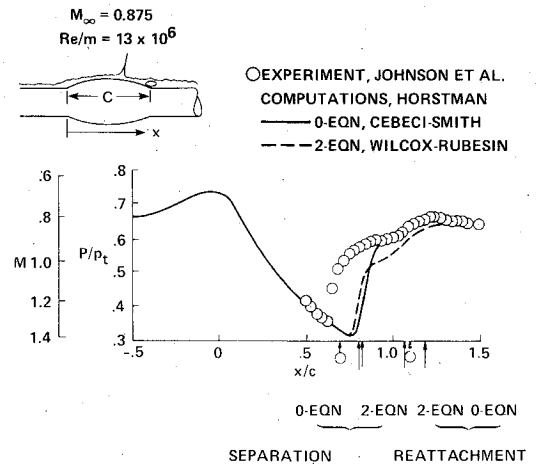

Fig. 11 Comparison of computation and experiment for an axisymmetric, transonic, shock-wave interaction: surface pressure and Mach number.

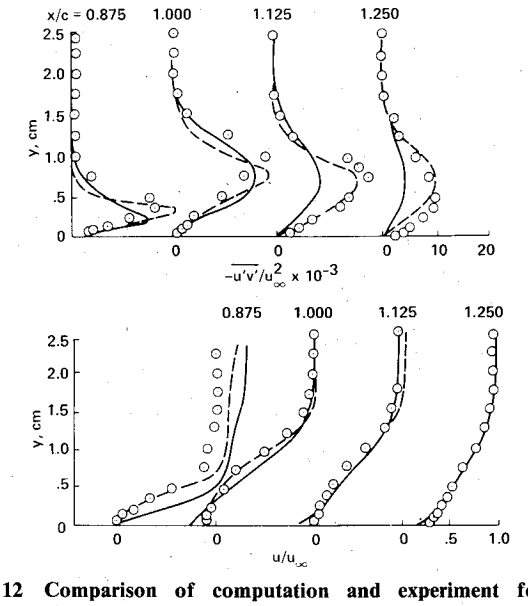

Fig. 12 Comparison of computation and experiment for an axisymmetric transonic shock-wave interaction: a) velocity profiles; and b) shear-stress profiles (see Fig. 11 for symbol notation).

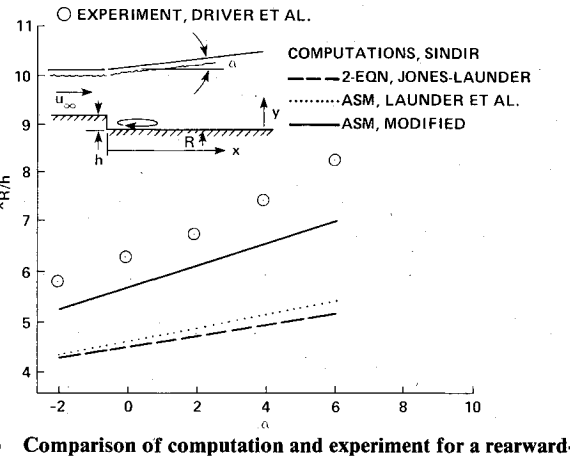

Fig. 13 Comparison of computation and experiment for a rearward-facing step: reattachment length.

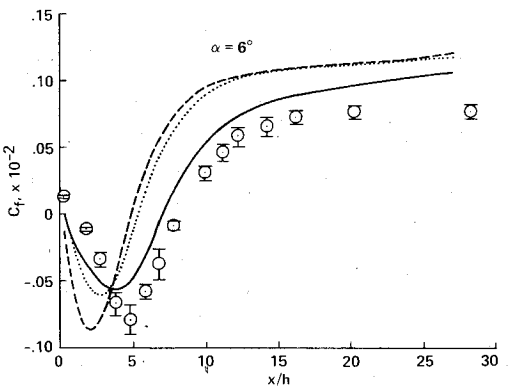

Fig. 14 Comparison of computation and experiment for skin friction on a rearward-facing step (see Fig. 13 for symbol notation).

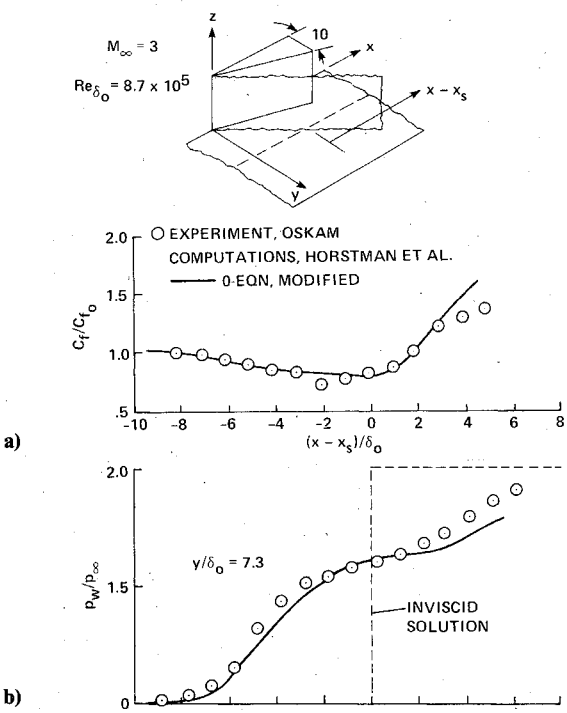

Fig. 15 Comparison of computation and experiment for a supersonic, swept shock-wave interaction: a) surface pressure; and b) skin friction.

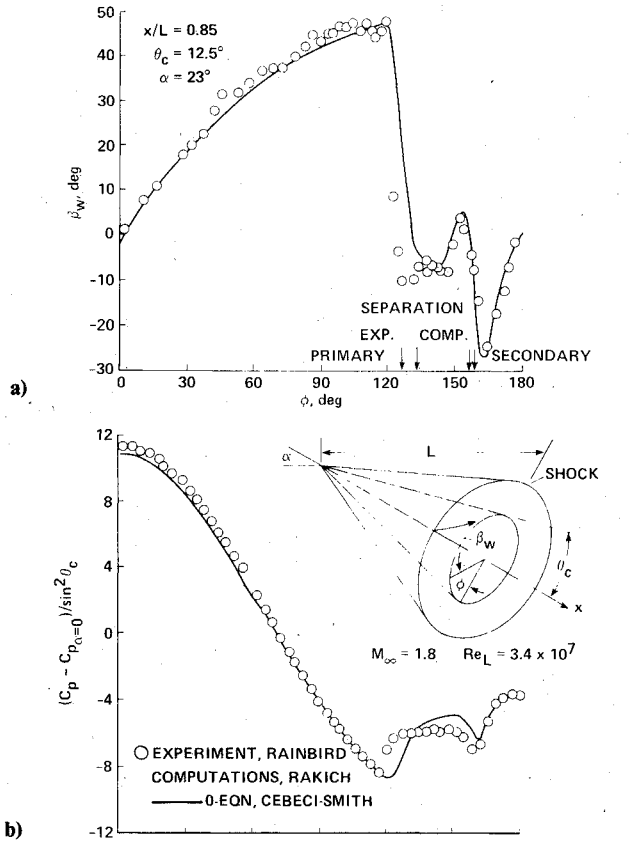

Fig. 16 Comparison of computation and experiment for a cone at high angle of attack: a) pressure coefficient; and b) wall shear-stress direction.

model, and that the two-equation model gives a better representation of the developing region in the vicinity of reattachment and beyond. Apparently, the computed results would be significantly better if the proper shock position could be predicted. It may be that eddy-viscosity concepts will have to be abandoned in favor of Reynolds-stress modeling for the region of the flow in the vicinity of the shock wave and for the recirculating region in the separated flow behind it.

Two-Dimensional Incompressible Flow: Fixed Separation

The behavior of the incompressible shear layer downstream of a rearward-facing step is similar to that found in the shear layer that develops downstream of a shock-induced separation on an airfoil.[62,63] However, in the case of the step, the separation point is fixed and the complicating presence of shock waves is absent. Hence, experimental and numerical studies are somewhat simpler and may provide some guidance for the more complicated problem. The geometry of a test flow under study[79] is sketched in Fig. 13. The angle of the upper wall can be varied to impose streamwise pressure gradients in the reattachment region and to move the reattachment point significantly. The reattachment length for a range of upper-wall angles is compared with computations.[82] Results for three turbulence models are shown. The predicted lengths using a two-equation, eddy-viscosity model and an algebraic stress model (ASM) are too small. Improvement was achieved, however, by modifying the stress model. The modification was made by rewriting the production term in the dissipation equation. The change in the production term causes dissipation to increase and shear stress to decrease, resulting in larger reattachment lengths. It is significant that similar modifications to the dissipation equation for the two-equation model had little effect on the prediction. This finding provided the basis of the argument for the need to abandon the eddy-viscosity concept in flows with large recirculating regions.[82] A comparison with the skin-friction data[79] for a deflected wall case in Fig. 14 shows similar improvements, as do velocity and shear-stress profile comparisons that are not shown here.

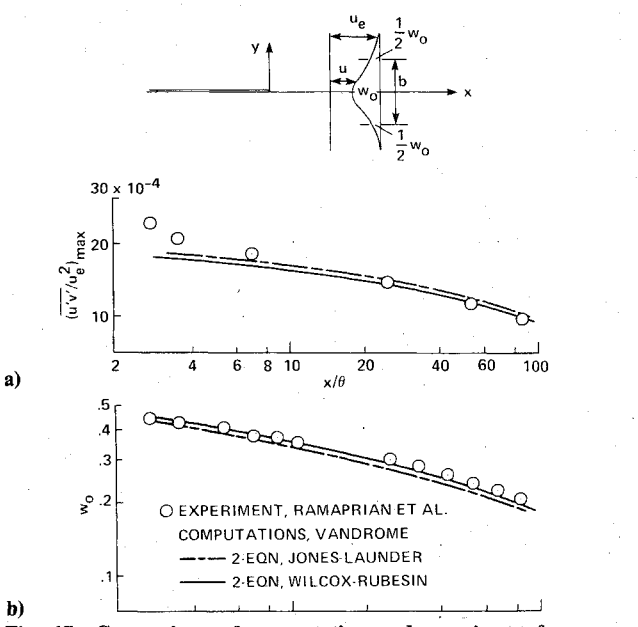

Fig. 17 Comparison of computation and experiment for a symmetric, incompressible wake without pressure gradient: a) centerline velocity defect; and b) maximum shear stress.

Two-Dimensional Incompressible Flow: Strong Adverse Pressure Gradient

In the cases in which there are adverse pressure gradients, the separation point may be unsteady, and its location depends on the extent of downstream separation, as it did for the shock-separated flows. The diffuser flow of Simpson et al.[83] was recommended as a test flow for evaluating modeling concepts for flows of this type.[9] However, reversed flow at

the downstream boundary makes it difficult to specify outflow boundary conditions. A few predictions have been reported. Zero-equation, eddy-viscosity models combined in interactive boundary-layer schemes were found to be fairly successful in calculating 1) the skin-friction distribution ahead of separation and 2) the location of the separation point itself, defined experimentally to be where flow reversal was measured at least 50% of the time. None of the computations predicts the flow downstream of separation.

Three-Dimensional Flows: Shock Waves

The swept shock wave impinging on a turbulent boundary layer is of interest in high-speed aerodynamic flows. A series of experiments and computations in the Mach number range between 2 and 6 has been reported.[84,85,88,89] An example (from Ref. 89) that illustrates the significant results from these studies is shown in Fig. 15. The computations use the time-averaged Navier-Stokes equations, with a zero-equation eddy-viscosity model modified[88] to account approximately for the flow in the corner formed at the intersection of the generator and the plate. Comparisons for the axial variation of pressure and skin friction show good agreement, even to the point of predicting the upstream influence of the shock wave on the boundary layer and the flow to within a boundary-layer thickness of the corner. Similar results are reported for the spanwise variation of pressure and heat transfer. Differences in the axial variations at the farthest downstream location are caused by locating the computational boundary there.

Good comparisons have also been reported for wedge angles to 12 deg and Mach numbers to 6. Such results are surprising in their contrast to those discussed previously for the two-dimensional impinging shock wave. The reason for this may be the absence of a recirculating flow region.

When a recirculating region is present behind a three-dimensional impinging shock, as was the case in the study of Kussoy et al.,[87] comparisons of computations and experiment result in conclusions similar to those drawn for the two-dimensional supersonic shock interactions discussed previously. Surface pressures are predicted well by eddy-viscosity models, but the stresses and flow angles in the viscous interaction regions of the flow are not.

Three-Dimensional High-Speed Flows: Cross Flow Separation

Studies of modeling for three-dimensional high-speed flows with cross flow separation on bodies of revolution at high angle of attack and supersonic speeds have begun recently. In Fig. 16, comparisons of computations[92] and experiment for a 12.5-deg cone at an angle of attack of 23 deg are shown. The experimental data[90] were evaluated and recommended for test flow purposes.[9] The computations are results of solutions to the Reynolds-averaged Navier-Stokes equations, reduced to parabolized form by neglecting derivatives of the stresses in the marching direction. A zero-equation, isotropic, eddy-viscosity model was used. The surface pressures are predicted fairly well, except between $\phi = 120$ and 160 deg, where primary and secondary cross flow separations are occurring. The flow-angle comparisons show that the primary separation line is predicted too far downstream, although the secondary separation and reattachment lines are in good agreement. There are larger discrepancies (not shown) between skin-friction predictions and data, especially between the locations of the leeward generator and the secondary separation point, where skin friction is underpredicted. Comparisons of the flow angles on the upper quadrant of the cone between the surface and the shock wave also suggest that the height of the cross flow separation region is underpredicted.

These results are similar to those for shock-separated, two-dimensional flows discussed previously, for which it was found that the eddy viscosities in the separated region were too large. McRae et al.[91] studied similar flows at lower angles of attack and used an anisotropic zero-equation, eddy-viscosity model. They chose to make the viscosity in the azimuthal direction less, by a ratio of 0.3, than the viscosity in the direction of the cone generator. Indeed, McRae et al. were able to show better agreement with the location of primary separation for one case. In another, they simply reduced the eddy viscosity in the separated region by 0.3. The significance of the study seems to be in the deduction that lower eddy viscosities in the cross flow separated region were needed to effect agreement. Obviously, more work is required to sort out the modeling problems. Nevertheless, the results, even using zero-equation, isotropic, eddy-viscosity models, indicate that it may now be possible to estimate pressure distributions and to give a qualitative representation of the lee flowfields for bodies of revolution at high angles of attack.

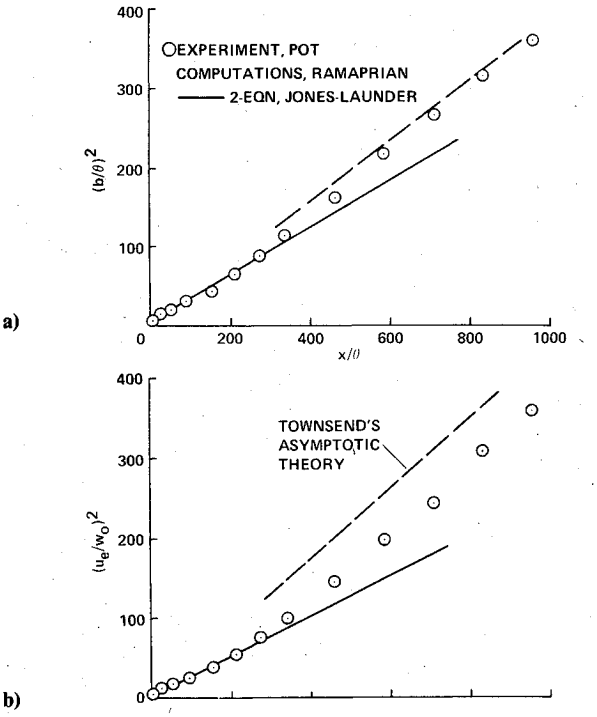

Fig. 18 Comparison of computation and experiment for a symmetric, incompressible wake without pressure gradient: a) centerline velocity defect; and b) wake half-thickness.

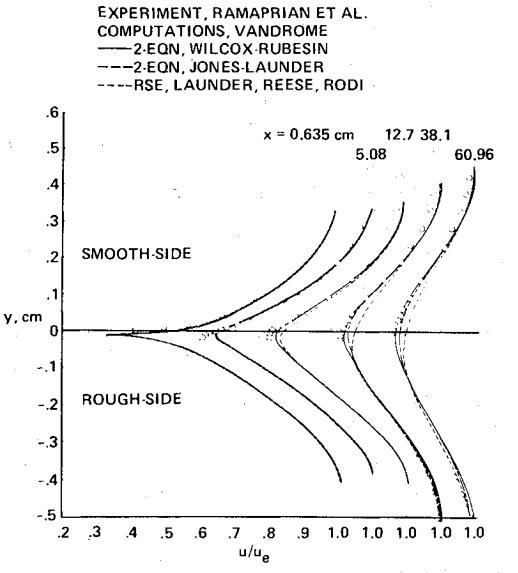

Fig. 19 Comparison of computation and experiment for an asymmetric incompressible wake without pressure gradient: velocity profiles.

Trailing-Edge Flows

Modeling of the flow near the trailing edge of a lifting surface is recognized as an important problem, especially at transonic speeds, because of its global effects on lift and drag.[108] The problem is complicated, because the abrupt change in boundary conditions causes substantial variation in the turbulent structure and because of viscid-inviscid interactions. The modeling status for this complex flow is discussed next.

Symmetric Flows: No Pressure Gradient

The wake behind a thin plate provides an idealized flow for studying the development of the turbulent structure. The wake can be thought of as consisting of three regions characterized by the level of mixing between the two individual boundary layers at the trailing edge.[93] In the first region (composed of about 25 momentum thicknesses θ), the development of an inner wake takes place as a result of the small-scale mixing of the two wall layers, while the outer velocity-defect layers remain practically unchanged. In the next region (out to a distance of about 350 θ), the influence of the wall becomes insignificant, and the wake evolves as a free turbulent flow with mixing between the outer layers. The final region is the asymptotic one where mixing is complete. For practical Reynolds numbers of interest in aerodynamic applications on lifting surfaces, the distance 1 chord from the trailing edge is equivalent to between 500 and 1000 θ. Thus, the first two regions are probably of most interest in aerodynamic applications.

The centerline velocity and the maximum shear stress measured downstream of a thin plate[93] are shown in Fig. 17. These data, within the developing region of a low-speed wake, are compared with unpublished calculations (D. Vandrome, Ames Research Center), in which two-equation eddy-viscosity models are used.[23,109] The predictions, using either model, provide a good representation of the velocity and shear-stress profile development, except that the initial values of maximum shear stress are underestimated—probably a result of the finite thickness of the experimental plate[93] and not of a model deficiency. Similar results of comparisons of the Andreopolous and Bradshaw[94] and Pot[96] experiments have also been reported.[93] Evidently, the development of the near-wake velocity and shear stress can be predicted satisfactorily by two-equation, eddy-viscosity models.

Predictions of the asymptotic regions of the wake are not satisfactory, however.[93] The velocity and wake half-thickness from the experiment of Pot[96] are compared with predictions in Fig. 18. Although the data follow the expected asymptotic behavior, the predictions do not, underestimating both the growth rate and defect-velocity parameter.

Asymmetric Flows: No Pressure Gradient

A more difficult test of the models occurs when two wall layers of different thickness merge at the trailing edge. Two experiments have been performed recently to help establish a physical description of the turbulent merging process and to test computations.[93,94] In each, one side was roughened to establish a thicker layer.

Experimental velocity and shear-stress profiles from Ref. 43 are compared in Figs. 19 and 20 with unpublished computations by Vandrome, using three turbulence models.[23,109,110]

The asymmetry of the velocity profiles is reproduced by the computations using any of the models, although on the rough side in the very near-wake, the predicted centerline velocity recovers more rapidly. This rapid recovery is a reflection of the overprediction of the magnitude of the viscous stresses there. Also, in the near-wake region the smooth-side shear-stress data show unusually high peaks that are not reflected in the computations. Experimentally, these are attributable to two factors: first, the presence of a finite-thickness trailing edge, which probably created a small region of reversed flow and subsequent vortical layer shedding; and second, the sudden removal of the viscous sublayer.[93] The computations cannot produce the first contribution because it is a parabolic scheme, but it does reflect the second, although how closely is a question that remains. The shear-stress model may perform somewhat better overall, but all of the models seem to do well enough for engineering estimates. Similar conclusions were reached during evaluation of predictions for the data of Ref. 94.

It should also be mentioned that Cebeci recently proposed a modification to the zero-equation, eddy-viscosity model for wake applications.[97] Comparisons with centerline velocity and wake-thickness parameters from Ref. 94 were reasonably good. The model requires a division of the wake into upper and lower halves and a specification of a length over which the viscosity changes to an asymptotic far-wake value. In the near-wake, inner region Cebeci assumes the velocity scale in the eddy viscosity to be the maximum friction velocity on the plate and the length scale to be proportional to a fraction of the displacement thickness, depending on the distance from the plate. Such a model is less general than the two-equation approach, because the position of the minimum wake velocity must be assumed along with the length of the near-wake region.

Based on the results of all the computations to date, eddy-viscosity models apparently do well enough in predicting most of the aerodynamic quantities of interest in the near-wake in the absence of pressure gradient; however, the issue of compressibility effects at Mach numbers above 1 is unresolved.

Symmetric Flow: Pressure Gradient

Adverse pressure gradients are usually present near the trailing edges of lifting surfaces. In such cases, especially at higher speeds, the importance of viscous-inviscid interaction emerges. To illustrate this, the displacement thicknesses from the test flow of Viswanath et al.[98] are compared (Fig. 21) with calculations using a Navier-Stokes code and a first-order boundary-layer code with the same turbulence model. Apparently, the Navier-Stokes calculation is better at the higher Mach number, because it includes the viscous-inviscid interaction as part of the solution.

Asymmetric Flow: Pressure Gradient

In a follow-on experiment, the wedge-shaped trailing edge was deflected 6 deg to create an asymmetric condition. One surface remained straight and a flat-plate type boundary layer developed on it. On the other, there was a severe adverse pressure gradient in the boundary layer. The merging of the two layers near the trailing edge and the wake was studied at Mach numbers of 0.4 and 0.6. Various computations were recently reported[9] for the lower Mach number case in which viscous-inviscid interaction is not important. The results of the mean-velocity and shear-stress profile comparisons are given in Fig. 22. Two of the predictions were obtained from solutions of the boundary-layer equations, and the same two-equation turbulence model (Jones-Launder). The third was obtained from the Reynolds-averaged, Navier-Stokes equations and a different two-equation model (Wilcox-Rubesin). As shown previously, model differences should have little influence in the wake region. However, one boundary-layer solution does not agree with the data on the wedge surface, where a strong pressure gradient exists. The influence of this initial disagreement persists downstream into the wake, illustrating the importance of initial conditions. In contrast, the other boundary-layer solution has a good match on the wedge, and the mean-velocity profile comparisons are quite adequate; however, the peak shear is underpredicted in the developing wake. The solution from the Navier-Stokes equations seems to be better overall, probably because the solution allows for slight normal pressure gradients near the trailing edge that affect the stresses developed.

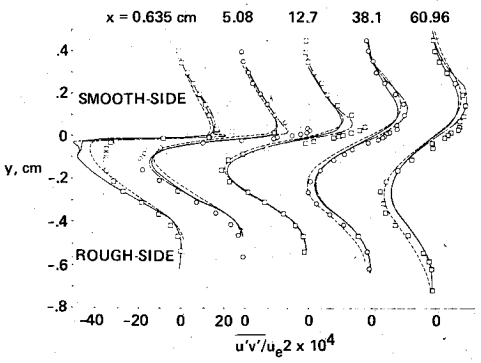

Fig. 20 Comparison of computation and experiment for an asymmetric incompressible wake without pressure gradient: shear profiles (see Fig. 19 for symbol notation).

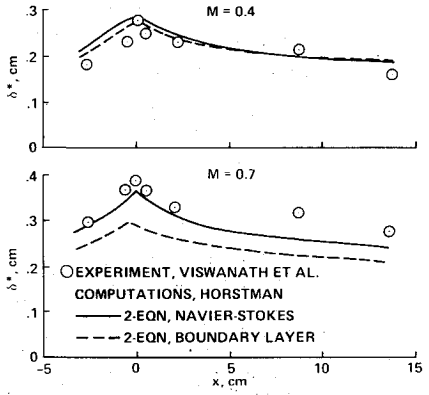

Fig. 21 Comparison of computation and experiment for a symmetric, trailing-edge flow with pressure gradient: displacement thickness.

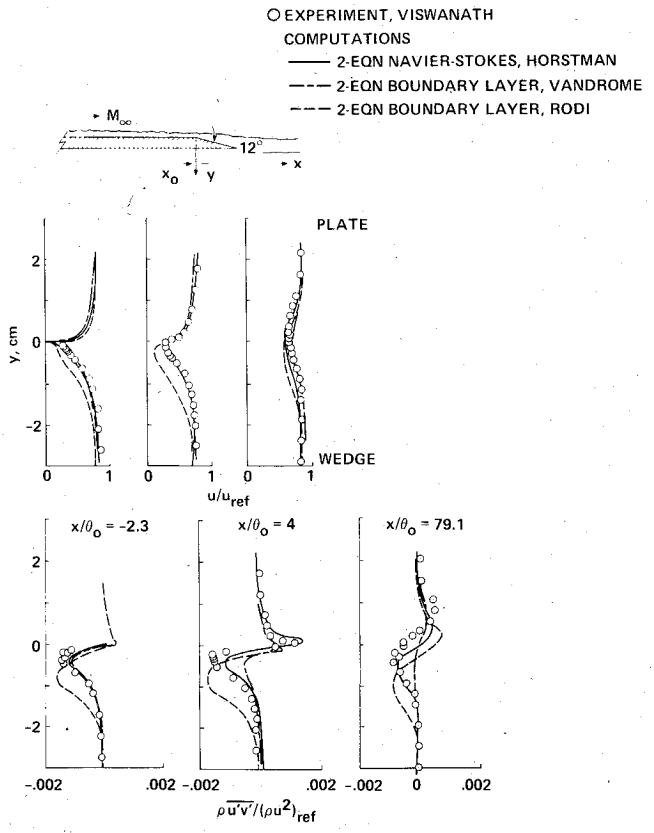

Fig. 22 Comparison of computation and experiment for an asymmetric, trailing-edge flow with pressure gradient, $M_\infty = 0.4$, $(\rho u^2)_{ref} = 0.7592 \times 10^5$ N/m², $u_{ref} = 153.6$ m/s; a) velocity profiles; and b) shear-stress profiles.

The development of the wake in the presence of pressure gradient is difficult to compute, and more work is required before definitive conclusions can be drawn. At this time it appears that eddy-viscosity concepts may be adequate for modeling these flows, provided viscous-inviscid interactions are accounted for.

Concluding Remarks

Attention has been directed to modeling within the framework of the Reynolds-averaged Navier-Stokes equations or their approximation. It was noted that for compressible flows, the form of these equations differs, depending on the averaging process. Favré-averaging, or mass-averaging, results in the most compact form, and it is the most popular for deriving the equations used to solve external aerodynamic flows. Regardless of the averaging process, compressibility has been included (only approximately) by introducing mean density into the velocity and length scales required in the modeling process. Apparently, this approximation works reasonably well for Mach numbers up to about 5 for attached flows.

The heuristic nature of modeling requires that it be guided and verified by experiment; there is a continuing need for more accurate data, and a framework wherein experiments are keyed directly to the stages of development of computational aerodynamics was introduced. The synergistic effect resulting from such a framework should accelerate the development process.

Modeling concepts were divided into two broad classes: eddy-viscosity and Reynolds-stress models. Distinguishing features between models of either class or between models within the same class arise through the particular closure technique that expresses the modeled quantities in terms of the mean-velocity field or in terms of the mean-turbulent field. The status of model development was reviewed by comparing computations with experimental data for three important flow regimes: attached, separated and reattaching, and trailing edge.

Modeling through eddy-viscosity concepts will probably be sufficient for most of the two-dimensional or axisymmetric attached flows of interest to aerodynamicists. As extra strain rates become more severe, those eddy-viscosity concepts that use solutions to the mean-turbulent-field equations are likely to provide better results. For three-dimensional, attached-flow applications, problems occur when large rates of skewing are present in boundary layers. For such cases, eddy-viscosity models are not adequate, and resorting to full Reynolds-stress models improves the picture only slightly.

At this stage of the development of computational aerodynamics for complex flows involving separation and strong viscous-inviscid interactions at trailing edges, it is exceedingly difficult to sort out discrepancies between computation and experiment that arise separately from modeling and computational procedures and from numerical errors. This situation will continue until computations can achieve grid-independence and until numerical smoothing procedures are understood more fully. Therefore, example comparisons of the type shown here and recently reported may not reflect the status of turbulence modeling alone. The question of modeling, then, is intertwined with numerical procedures, and the conclusions we have drawn will have to be viewed in that light. For test flows with shock-induced separation, in which the shock position is fixed by geometry or external constraints, and in which the separated region is confined to several boundary-layer thicknesses, pressure distributions are predicted reasonably well by numerical procedures that use eddy-viscosity models. This means, for example, that one could predict control-surface aerodynamic effectiveness with reasonable certainty. On the other hand, skin friction and heat transfer in the recirculating regions are not predicted, although some improvement can be achieved,

especially in the developing regions downstream, when closure is accomplished by solving mean-turbulent-field equations. For transonic flows in which strong shocks and separation are present, shock-wave position cannot be predicted with these same eddy-viscosity models; hence, neither lift nor drag on an airfoil can be estimated accurately. Evidently in these situations, the elliptic character of the flow required adequate modeling of all viscous regions downstream. It may be necessary to resort to Reynolds-stress modeling, but this will be costly in terms of computational efficiency. Although the situation for three-dimensional separated flow is not much different, the results for the swept-shock test flows, in which no region of recirculation exists, are encouraging. Evidently—for a practical range of Mach numbers and Reynolds numbers—pressure, skin friction, and heat transfer may all be obtained with accuracy suitable for engineering purposes, using numerical procedures that use algebraic eddy-viscosity models. Symmetric and asymmetric, two-dimensional, near-wake flows can probably be calculated with eddy-viscosity models too, as long as the Mach number is subsonic. However, on lifting surfaces where pressure gradients are present, it may be necessary to include viscous-inviscid interaction effects in the numerical procedures.

No single turbulence model emerges that applies generally to the variety of flows encountered in computational aerodynamics; thus, turbulence modeling remains an important pacing item. In the near future, research within the framework of the Reynolds-averaged Navier-Stokes equations will likely be directed toward developing more accurate numerical procedures coupled with turbulence models, which together will be "tuned" for solving specific flow classes, such as those discussed in this paper. A broader data base and attention to data accuracy will be necessary to guide and verify this effort, especially for three-dimensional flows.

Acknowledgments

The author wishes to express sincere gratitude to his coworkers in the Experimental Fluid Dynamics Branch, Ames Research Center, whose research activities comprise a major portion of the material used in this paper. He further acknowledges the help of many others who willingly supplied information on their current research; their cooperation served to broaden the perspective of this paper.

References

[1] Chapman, D. R., "Computational Aerodynamics—Development and Outlook," *AIAA Journal,* Vol. 17, Dec. 1979, pp. 1293-1313.

[2] Reinecke, G., "Forecasting the 80's," *Astronautics & Aeronautics,* Vol. 19, July/Aug. 1981, pp. 46-47.

[3] Chapman, D. R., "Trends and Pacing Items in Computational Aerodynamics," *Seventh International Conference on Numerical Methods in Fluid Dynamics, Lecture Notes in Physics,* Springer-Verlag, N.Y., 1981.

[4] Reynolds, O., "On the Dynamical Theory of Incompressible Viscous Fluid and the Determination of the Criterion," *Philosophical Transactions of the Royal Society of London, Series A,* Vol. 186, (Papers 2 and 535), 1874, pp. 123-161.

[5] Laufer, J., "New Trends in Experimental Turbulence Research," *Annual Review of Fluid Mechanics, Vol. 7,* Annual Review, Palo Alto, Calif., 1975, pp. 307-329.

[6] Moin, P. and Kim, J., "Large Scale Numerical Simulation of Wall-Bounded Turbulent Shear Flows," NASA TM-81309, 1981.

[7] Rogallo, R., "Direct Simulation of Homogeneous Turbulence at Low Reynolds Numbers," NASA TM-81315, 1981.

[8] Kline, S. J., et. al., *Proceedings of the AFOSR-IFP-Stanford Conference on Computation of Turbulent Boundary Layers,* Vols. I and II, Stanford Univ., Stanford, Calif., Aug. 1968.

[9] Kline, S. J., Cantwell, B. J., and Lilley, G. M. eds., *The 1980-81 AFOSOR-HTTM-Stanford Conference on Complex Turbulent Flows: Comparison of Computation and Experiment,* Vol. I 1981, Vol. II 1982, Vol. III 1981. Published and distributed by Thermophysics Div., Mech. Engr. Dept., Stanford Univ., Stanford, Calif.

[10] Launder, B. E. and Spalding, D. B., *Mathematical Models of Turbulence,* Academic Press, New York, 1972.

[11] Cebeci, T. and Smith, A. M. O., *Analysis of Turbulent Boundary Layers,* Academic Press, New York, 1974.

[12] Bradshaw, P., Cebeci, T., and Whitelaw, J., *Engineering Calculation Methods for Turbulent Flow,* Academic Press, New York, 1981.

[13] Donaldson, C. duP. and Sullivan, R. D., "An Invariant Second-Order Closure Model of the Compressible Turbulent Boundary Layer on a Flat Plate," Aeronautical Research Associates of Princeton, Inc., Princeton, N.J., Rept. 178, June 1972.

[14] Rubesin, M. W. and Rose, W. C., "The Turbulent Mean Flow Reynolds-Stress and Heat Flux Equations in Mass-Averaged Dependent Variables," NASA TM X-62,248, 1973.

[15] Boussinesq, J., "Theorie de l'ecoulement tourbillant," *Memoires Presentes par Divers Savants Sciences Mathématique at Physiques, Académie des Sciences,* Paris, France, Vol. 23, 1877, p. 46.

[16] Reynolds, W. C., "Computation of Turbulent Flows," Thermosciences Division, Dept. of Mechanical Engineering, Stanford Univ., Stanford, Calif., Rept. TF-4, 1975.

[17] Morkovin, M. V., "Effects of Compressibility on Turbulent Flows," *The Mechanics of Turbulence,* Fordon and Breach, New York, 1961, p. 367.

[18] Wilcox, D. C. and Alber, I. E., "A Turbulence Model for High Speed Flows," *Proceedings of the 23rd Heat Transfer and Fluid Mechanics Institute,* Northridge, Calif., June 14-16, 1972, pp. 231-252.

[19] Rubesin, M. W., "A One-Equation Model of Turbulence for Use with the Compressible Navier-Stokes Equations," NASA TM X-73128, 1976.

[20] Coakley, T. J. and Viegas, J. R., "Turbulence Modeling of Shock Separated Boundary Layer Flows," Symposium on Turbulent Shear Flows, University Park, Pa., April 18-20, 1977.

[21] Bradshaw, P., Ferris, D. H., and Atwell, N. P., "Calculation of Boundary Layer Development Using the Turbulent Energy Equation," *Journal of Fluid Mechanics,* Vol. 28, 1967, p. 593.

[22] Rodi, W., "Turbulence Models and Their Application in Hydraulics, a State-of-the-Art Review," International Association of Hydraulic Research, Delft, the Netherlands, June 1980.

[23] Wilcox, D. C. and Rubesin, M. W., "Progress in Turbulence Modeling for Complex Flow Fields Including the Effects of Compressibility," NASA TP-1517, 1980.

[24] Marvin, J. G., "Advancing Computational Aerodynamics through Wind-Tunnel Experimentation," AGARD Fluid Dynamics Panel Meeting on Integration of Computers and Wind Tunnel Testing, Chattanooga, Tenn., Sept. 24-25, 1980.

[25] Van Driest, E., "Turbulent Boundary Layer in Compressible Fluids," *Journal of the Aerospace Sciences,* Vol. 18, No. 3, 1951, pp. 145-160.

[26] Fernholz, H. H. and Finley, P. J., "A Critical Compilation of Compressible Turbulent Boundary Layer Data," AGARDograph 223, June 1977.

[27] Rubesin, M. W., Crisalli, A. J., Lanfranco, M. D., Horstman, C. C., and Acharya, M., "A Critique of Some Recent Second-Order Turbulence Closure Models for Compressible Boundary Layers," AIAA Paper 77-128, Los Angeles, Calif., 1977.

[28] Wilcox, D. C. and Traci, R. M., "A Complete Model of Turbulence," AIAA Paper 76-351, San Diego, Calif., 1976.

[29] Horstman, C. C., Kussoy, M. I., and Lanfranco, M. J., "An Evaluation of Several Compressible Turbulent Boundary Layer Models: Effects of Pressure Gradient and Reynolds Number," AIAA Paper 78-1160, Seattle, Wash., 1978.

[30] Kussoy, M. I., Horstman, C. C., and Acharya, M., "An Experimental Documentation of Pressure Gradient and Reynolds Number Effects on Compressible Turbulent Boundary Layers," NASA TM X-78488, 1978.

[31] Jobe, C. E. and Hankey, W. L., "Turbulent Boundary Layer Calculations in Adverse Pressure Gradient Flows," AIAA Paper 80-0136, Pasadena, Calif., 1980.

[32] Horstman, C. C., "A Turbulence Model for Nonequilibrium Adverse Pressure Gradient Flows," AIAA Paper 76-412, San Diego, Calif., 1976.

[33] Parikh, P. G., Kays, W. M., and Moffat, R. J., "A Study of Adverse Pressure Gradient Turbulent Boundary Layers with Outer Region Non-Equilibrium," Thermosciences Division, Stanford Univ., Stanford, Calif., Rept. HMT-26, July 1976.

[34] So, R. M. C. and Mellor, G. C., "An Experimental Investigation of Turbulent Boundary Layers along Curved Surfaces," NASA CR-1940, 1972.

[35] Laderman, A. J., "Pressure Gradient Effects on Supersonic Boundary-Layer Turbulence," Ford Aeronutronics Division,

Newport Beach, Calif., Rept. U6467, Oct. 1978; also AIAA Paper 79-1563, July 1979.

[36] Eide, S. A. and Johnston, J. P., "Prediction of Effects of Longitudinal Wall Curvature and System Rotation on Turbulent Boundary Layers," Department of Mechanical Engineering, Stanford Univ., Stanford, Calif., Rept. PD-19, 1974.

[37] Cebeci, T., Hirsh, R. S., and Whitelaw, J. H., "On the Calculation of Laminar and Turbulent Boundary Layers on Longitudinally Curved Surfaces," *AIAA Journal,* Vol. 17, April 1979, p. 434.

[38] Bradshaw, P., "Effects of Streamline Curvature on Turbulent Flow," AGARDograph 169, 1973.

[39] Elsenaar, A., van den Berg, B., and Lindhout, J. P. F., "Three-Dimensional Separation of an Incompressible Turbulent Boundary Layer on an Infinite Swept Wing," *Flow Separation,* AGARD CP-168, 1975, pp. 34-1 to 34-10.

[40] Humphreys, D. A. (Ed.), *Stockholm Workshop of EUROVISC Working Party, PT1/15-Wing,* The Aeronautical Research Institute of Sweden, Stockholm, FFA-TN, 1978.

[41] East, L. F., "Measurements of the Three-Dimensional Incompressible Turbulent Boundary Layer Induced on the Surface of a Slender Delta Wing by the Leading Edge Vortex," RAE Tech. Rept. 73141, 1974.

[42] Lemmerman, L. A. and Burdges, K. P., "Three Dimensional Boundary Layer on a Finite, Swept Wing: Measurements and Comparisons with Computations," Presented at U.S.-German Data Exchange Meeting, DFVLR-AVA, Göttingen, Germany, April 28-30, 1981.

[43] East, L. F. and Hoxey, R. P., "Low-Speed Turbulent Boundary-Layer Data, Part I," RAE, Farnborough, England, TR 69041, March 1969.

[44] Müller, R. R., "Mean Velocities and Reynolds Stresses Measured in a Three-Dimensional Boundary Layer," *Viscous and Interacting Flow Field Effects,* 5th U.S. Air Force and the Federal Republic of Germany Data Exchange Agreement Meeting, AFWAL-TR-80-3088, 1980.

[45] Cousteix, J., Aupoix, B., and Pailhas, G., "Synthese de resultats theoriques et experimentaux sur les couches limites et sillages turbulents tridimensionnels," Office National d'Etudes et de Recherches Aerospatiales, Paris, France, ONERA-NT-1980-4, 1980.

[46] East, L. F. (Ed.), "Computation of Three-Dimensional Turbulent Boundary Layers—Using Integral and Differential Prediction Methods," The Aeronautical Research Institute of Sweden, Stockholm, FFA-TN-AE-1211, 1975.

[47] Krause, E., "Strive for Accuracy—Improvement of Predictions," *Computers and Fluids,* Vol. 8, 1980.

[48] Higuchi, H. and Rubesin, M., "An Experimental and Computational Investigation of the Transport of Reynolds Stresses in an Axisymmetric Swirling Boundary Layer," AIAA Paper 81-0416, St. Louis, Mo., 1981.

[49] Schneider, G. R., "Calculation of Three-Dimensional Boundary Layers on Bodies of Revolution at Incidence," *Viscous and Interacting Flow Field Effects, Proceedings of the 5th U.S. Air Force and the Federal Republic of Germany Data Exchange Agreement Meeting,* edited by A. F. Fiore, AFWAL-TR-80-3088, 1980.

[50] Rotta, J. C., "A Family of Turbulence Models for Three-Dimensional Boundary Layers," *Proceedings of the First Symposium on Turbulent Shear Flows,* edited by F. Durst, B. E. Launder, F. W. Schmidt, and J. H. Whitelaw, Springer-Verlag, Berlin/Heidelberg/New York, 1979.

[51] Bradshaw, P. and Terrell, M. G., "The Response of a Turbulent Boundary Layer on an Infinite Swept Wing to the Sudden Removal of Pressure Gradient," National Physical Laboratory, Teddington, England, NPL Aero Rept. 1305, 1969.

[52] Rotta, J. C., "On the Effect of the Pressure Strain Correlations on the Three-Dimensional Turbulent Boundary Layers," 2nd Symposium on Turbulent Shear Flows, London, 1979.

[53] Bertelrud, A., Bergmann, M. Y., and Coakley, T. J., "Experimental and Computational Study of Transonic Flow About Swept Wings," AIAA Paper 80-0005, Pasadena, Calif., 1980.

[54] Sturek, W. B. and Schiff, L. B., "Computations of the Magnus Effect for Slender Bodies in Supersonic Flow," AIAA Paper 80-1586, *Proceedings of the AIAA Atmospheric Flight Mechanics Conference,* 1980, pp. 260-270.

[55] Schiff, L. B. and Sturek, W. B., "Numerical Simulation of Steady Supersonic Flow over an Ogive-Cylinder-Boattail Body," AIAA Paper 80-0066, Pasadena, Calif., 1980.

[56] Kordulla, W., "Investigations Related to the Inviscid-Viscous Interaction in Transonic Flows About Finite 3-D Wings," *AIAA Journal,* Vol. 16, 1978, pp. 369-376.

[57] Kussoy, M. I. and Horstman, C. C., "An Experimental Documentation of a Hypersonic Shock-Wave Turbulent Boundary Layer Interaction Flow—With and Without Separation," NASA TM X-62,412, 1975.

[58] Holden, M. S., "Shock Wave-Turbulent Boundary-Layer Interaction in Hypersonic Flow," AIAA Paper 72-74, San Diego, Calif., Jan. 1972.

[59] Redda, D. C. and Murphy, J. D., "Shock Wave Turbulent Boundary-Layer Interaction in Rectangular Channels. Part II: The Influence of Sidewall Boundary-Layers on Incipient Separation and Scale of Interaction," *AIAA Journal,* Vol. 11, Oct. 1973, pp. 1367-1368.

[60] Johnson, D. A., Horstman, C. D., and Bachelo, W. D., "A Comprehensive Comparison between Experiment and Prediction for a Transonic Turbulent Separated Flow," AIAA Paper 80-1407, Snowmass, Colo., 1980.

[61] McDevitt, J. B., Levy, L. L. Jr., and Deiwert, G. S., "Transonic Flow About a Thick Circular-Arc Airfoil," *AIAA Journal,* Vol. 14, May 1976, pp. 606-613.

[62] Seegmiller, H. L., Marvin, J. G., and Levy, L. L. Jr., "Steady and Unsteady Transonic Flows," *AIAA Journal,* Vol. 16, Dec. 1978, pp. 1262-1270.

[63] Delery, J. M., "Investigation of Strong Shock Turbulent Boundary Layer Interaction in 2-D Transonic Flows with Emphasis on Turbulence Phenomena," AIAA Paper 81-1245, Palo Alto, Calif., 1981.

[64] Mateer, G. C. and Viegas, J. R., "Effect of Mach Number and Reynolds Number on a Normal Shock-Wave/Turbulent Boundary Layer Interaction," AIAA Paper 79-1502, Williamsburg, Va., 1979.

[65] Settles, G. S., Vas, I. E., and Bogdonoff, S. M., "Details of a Shock-Separated Turbulent Boundary Layer at a Compression Corner," *AIAA Journal,* Vol. 14, Dec. 1976, pp. 1709-1715.

[66] LeBalleur, J. C., Peyret, R., and Viviand, H., "Numerical Studies in High Reynolds Number Aerodynamics," *Computers and Fluids,* Vol. 8, March 1980, pp. 1-30.

[67] Carter, J. E., "Viscous-Inviscid Interaction Analysis of Transonic Turbulent Separated Flow," AIAA Paper 81-1241, Palo Alto, Calif., 1981.

[68] Marvin, J. G., Horstman, C. C., Rubesin, M. W., Coakley, T. J., and Kussoy, M. I., "An Experimental and Numerical Investigation of Shock-Wave Induced Turbulent Boundary Layer Separation at Hypersonic Speeds," AGARD-CCP 168, May 1975.

[69] Baldwin, B. S. and MacCormack, R. W., "Numerical Solution of a Strong Shock Wave With a Hypersonic Turbulent Boundary Layer," AIAA Paper 74-558, Palo Alto, Calif., 1974.

[70] Baldwin, B. S. and Rose, W. C., "Calculation of Shock-Separated Turbulent Boundary Layers," Conference on Aerodynamic Analysis Requiring Advanced Computers, Langley, Va., NASA SP-347, March 4-6, 1975.

[71] Deiwert, G. S., "Computation of Separated Transonic Flows," *AIAA Journal,* Vol. 14, June 1976, pp. 735-740.

[72] Viegas, J. R. and Horstman, C. C., "Comparison of Multiequation Turbulence Models for Several Shock Separated Boundary Layer Interaction Flows," AIAA Paper 78-1165, Seattle, Wash., 1978.

[73] Coakley, T. J., Viegas, J. R., and Horstman, C. C., "Evaluation of Turbulence Models for Three Primary Types of Shock Separated Boundary Layers," AIAA Paper 77-692, Albuquerque, N. Mex., 1977.

[74] Shang, J. S., Hankey, W. L. Jr., and Law, H. C., "Numerical Simulation of Shock-Wave-Turbulent Boundary-Layer Interaction," *AIAA Journal,* Vol. 14, Oct. 1976, p. 1451.

[75] Coakley, T. J. and Bergmann, M. Y., "Effects of Turbulent Model Selection on Prediction of Complex Aerodynamic Flows," AIAA Paper 79-0070, New Orleans, La., 1979.

[76] Coakley, T. J., "Numerical Method for Gas Dynamics Combining Characteristics and Conservation Concepts," AIAA Paper 81-1257, Palo Alto, Calif., 1981.

[77] Liou, M. S., Coakley, T. J., and Bergmann, M. Y., "Numerical Simulation of Transonic Flows in Diffusers," AIAA Paper 81-1240, Palo Alto, Calif., 1981.

[78] Kim, J., Kline, S. J., and Johnston, J. P., "Investigation of Separation and Reattachment of a Turbulent Shear Layer: Flow Over a Backward Facing Step," Dept. of Mechanical Engineering, Stanford Univ., Stanford, Calif., Rept. MD 37, 1978.

[79] Driver, D. M. and Seegmiller, H. L., "Features of a Reattaching Turbulent Shear Layer Subject to an Adverse Pressure," AIAA Paper 82-0102, St. Louis, Mo., June 1982.

[80] Viswanath, P. R. and Brown, J. L., "Separated Trailing-Edge Flow at a Transonic Mach Number," AIAA Paper 82-0348, Orlando, Fla., 1982.

[81] Smith, A. M. O., "Remarks on the Fluid Mechanics of the Stall," AGARD-LS-74, Feb. 1975.

[82] Sindir, M., "Study of Turbulent and Laminar Recirculating Flows in a Backward-Facing Step Geometry," Dissertation, Mechanical Engineering Dept., Univ. of California at Davis, July 1982.

[83] Simpson, R. L., Chew, Y.-T., and Shwaprassad, B. G., "Measurements of a Separating Turbulent Boundary Layer," Southern Methodist Univ., Dallas, Texas, Project SQUID Rept. SMU-4-PU, 1980.

[84] Peak, D. J., "Three Dimensional Swept Shock/Turbulent Boundary Layer Separation with Control of Air Injection," National Research Council-Canada, Aeronautical Rept. L.R. 592, July 1976.

[85] Oskam, B., Bogdonoff, S. M., and Vas, I. E., "Study of Three-Dimensional Flow Fields Generated by the Interaction of a Skewed Shock Wave with a Turbulent Boundary Layer," AFFDL-TR 75-21, WPAFB, Feb. 1975.

[86] Shang, J. S., Hankey, W. L., and Patty, J. S., "Three Dimensional Supersonic Interacting Turbulent Flow along a Corner," *AIAA Journal,* Vol. 17, July 1979, pp. 706-713.

[87] Kussoy, M. I., Horstman, C. C., and Viegas, J. R., "An Experimental and Numerical Investigation of a Three-Dimensional Shock Separated Turbulent Boundary Layer," *AIAA Journal,* Vol. 18, Dec. 1980, pp. 1477-1484.

[88] Hung, C. M. and MacCormack, R. W., "Numerical Solution of Three-Dimensional Shock Wave and Turbulent Boundary Layer Interaction," *AIAA Journal,* Vol. 16, Oct. 1978, pp. 1090-1096.

[89] Horstman, C. C. and Hung, C. M., "Computation of Three Dimensional Turbulent Separated Flows at Supersonic Speeds," AIAA Paper 79-0002, New Orleans, La., 1979.

[90] Rainbird, W. J., "Turbulent Boundary Layer Growth and Separation on a Yawed Cone," *AIAA Journal,* Vol. 6, 1968, p. 2410; see also AGARD CP 30, 1968.

[91] McRae, D. S., Peake, D. J., and Fisher, D. F., "A Computational and Experimental Study of High Reynolds Number Viscous/Inviscid Interaction about a Cone at High Angle of Attack," AIAA Paper 80-1422, Snowmass, Colo., 1980.

[92] Rakich, J. V., Davis, R. T., and Barnett, M., "Simulation of Large Turbulent Structures with the Parabolic Navier-Stokes Equations," Eighth International Conference on Numerical Methods in Fluid Dynamics, Aachen, FRG, June 1982.

[93] Ramaprian, B. R., Patel, V. C., and Sastry, M. S., "Turbulent Wake Development behind Streamlined Bodies," Iowa Institute of Hydraulic Research, Univ. of Iowa, Iowa City, Iowa, IIHR Rept. 231, July 1981.

[94] Andreopolous, J. and Bradshaw, P., "Measurement of Interacting Turbulent Shear Layers in the Near Wake of a Flat Plate," *Journal of Fluid Mechanics,* Vol. 100, 1980, pp. 639-668.

[95] Luechter, O., "Effects of Freestream Turbulence and Initial Boundary Layers on the Development of Turbulent Mixing Layers," *A Project Squid Workshop on Turbulence in Internal Flows,* edited by S. N. B. Murthy, Hemisphere Publishing Corp., Wash., London, 1977, pp. 371-401.

[96] Pot, P. J., "Measurements in a 2-D Wake Merging into a Boundary Layer," National Aerospace Laboratory, the Netherlands, Data Rept. NLR TR-79063L, 1979.

[97] Cebeci, T. and Meier, H. V., "Modeling Requirements for the Calculation of the Turbulent Flow Around Airfoils, Wings and Bodies of Revolution," Paper 16, AGARD-CP-271, 1980.

[98] Viswanath, P. R., Cleary, J. W., Seegmiller, H. L., and Horstman, C. C., "Trailing Edge Flows at High Reynolds Number," *AIAA Journal,* Vol. 18, Sept. 1980, pp. 1059-1065.

[99] Cleary, J. W., Viswanath, P. R., Horstman, C. C., and Seegmiller, H. L., "Asymmetric Trailing-Edge Flows at High Reynolds Number," AIAA Paper 80-1369, Snowmass, Colo., 1980.

[100] Spaid, F. W. and Stivers, L. S. Jr., "Supercritical Airfoil Boundary Layer Measurements," AIAA Paper 79-1501, Williamsburg, Va., 1979.

[101] Johnson, D. A. and Spaid, F. W., "Measurements of the Boundary Layer and Near Wake of a Supercritical Airfoil at Cruise Conditions," AIAA Paper 81-1241, Palo Alto, Calif., 1981.

[102] Baker, A. J., "Prediction and Measurement of Turbulent Aerodynamic Trailing Edge Flows," AIAA Paper 80-1395, Snowmass, Colo., 1980.

[103] Olson, L. E. and Orloff, F. L., "On the Structure of Turbulent Wakes and Merging Shear Layers of Multielement Airfoils," AIAA Paper 81-1238, Palo Alto, Calif., 1981.

[104] Cook, T. A., "Measurements of the Boundary Layer and Wake of Two Aerofoil Sections at High Reynolds Number and High Subsonic Mach Numbers," RAE Tech Rept. 71127, 1971.

[105] Deiwert, G. S., "Computation of Turbulent Near Wake for Asymmetric Airfoils," NASA TM-78581, 1979.

[106] MacCormack, R. W., "Numerical Solution of the Interaction of a Shock Wave with a Laminar Boundary Layer," *Lecture Notes in Physics,* Vol. 8, Springer-Verlag, New York, 1971, p. 151.

[107] Baldwin, B. S. and Lomax, H., "Thin Layer Approximation and Algebraic Model for Separated Turbulent Flows," AIAA Paper 78-257, Huntsville, Ala., 1978.

[108] Melnik, R. E., Chow, R., and Mead, H. R., "Theory of Viscous Transonic Flow over Airfoils at High Reynolds Number," AIAA Paper 77-680, Albuquerque, N. Mex., 1977.

[109] Jones, W. P. and Launder, B. E., "The Prediction of Laminarization with a Two-Equation Model of Turbulence," *International Journal of Heat and Mass Transfer,* Vol. 15, 1971, pp. 301-314.

[110] Launder, B. E., Reese, G. J., and Rodi, W., "Progress in the Development of a Reynolds Stress Turbulence Closure," *Journal of Fluid Mechanics,* Vol. 68, 1975, pp. 537-566.